Sanger, F., Nicklen, S., & Coulson, A. R. (1977) *Proc. Natl. Acad. Sci. U.S.A. 74*, 5463-5467.
Scanu, A. M., & Fless, G. M. (1990) *J. Clin. Invest. 85*, 1709-1715.
Seed, M., Hoppichler, F., Reaveley, D., McCarthy, S., Thompson, G. R., Boerwinkle, E., & Utermann, G. (1990) *New Engl. J. Med. 322*, 1494-1499.
Seki, T., Hagiya, M., Shimohishi, M., Nakamura, T., & Shimizu, S. (1991) *Gene 102*, 213-219.
Silhavy, T. J., Berman, W. L., & Enquist, L. W. (1984) in *Experiments with Gene Fusions*, pp 140-141, Cold Spring Harbor Laboratory, New York.
Utermann, G. (1989) *Science 246*, 904-910.
Utermann, G., Menzel, H. J., Kraft, H. G., Duba, H. C., Kemmler, H. G., & Seitz, C. (1987) *J. Clin. Invest. 80*, 458-465.
Yoshitake, S., Schach, B. G., Foster, D. C., Davie, E. W., & Kurachi, K. (1985) *Biochemistry 24*, 3736-3750.

Deuterium Exchange of Operator 8CH Groups as a Raman Probe of Repressor Recognition: Interactions of Wild-Type and Mutant λ Repressors with Operator O_L1†

Kim E. Reilly, Renee Becka, and George J. Thomas, Jr.*
Division of Cell Biology and Biophysics, School of Basic Life Sciences, University of Missouri—Kansas City, Kansas City, Missouri 64110

Received November 1, 1991; Revised Manuscript Received January 7, 1992

ABSTRACT: The rate of deuterium exchange of a purine 8CH group in DNA is highly sensitive to both macromolecular secondary structure and intermolecular interactions which restrict solvent access to the major groove [Lamba, O. P., Becka, R., & Thomas, G. J., Jr. (1990) *Biopolymers 29*, 1465-1477]. We have exploited the sensitivity of the 8CH → 8CD reaction to probe DNA recognition by the helix-turn-helix (HTH) motif of phage λ cI repressor. We find that purine exchanges in the 19-base-pair O_L1 operator are strongly and specifically restricted by binding of the HTH N-terminal domain of the repressor fragment (RF) comprising residues 1-102. The kinetics indicate large-scale obstruction of solvent access to operator 7N-8C purine sites. Interpretation of the exchange kinetics using a simple model suggests that only 7 purine residues (5 of 10 adenines and 2 of 9 guanines) remain unrestricted with respect to 8CH exchange in complexes of O_L1 with the wild-type repressor. On the other hand, the 8CH exchange profile for the complex of O_L1 with the Tyr88→Cys mutant repressor indicates that 9 purines (7 adenines and 2 guanines) are exchangeable. These results suggest important differences in major groove recognition in the two complexes. The proposed 8CH labeling profiles are consistent with molecular models of related complexes determined by X-ray crystallography [Jordan, S. R., & Pabo, C. O. (1988) *Science 242*, 893-899] and indicate that the structures observed in the crystal are largely maintained in solution. The results also implicate both steric shielding of the 7N-8C locus and specific hyrogen bonding to the 7N acceptor by repressor donor groups as factors which contribute to retardation of operator 8CH exchange. Finally, present results confirm for D_2O solutions of repressors, operators, and complexes the same secondary structures and thermostabilities reported previously for corresponding H_2O solutions [Benevides, J. M., Weiss, M. A., & Thomas, G. J., Jr. (1991) *Biochemistry 30*, 4381-4388, 5955-5963].

The control of gene expression in prokaryotic and eukaryotic cells requires recognition of discrete DNA-binding domains by regulatory proteins. An intensively studied example is the cI repressor-operator system of bacteriophage λ (Ptashne, 1986). The N-terminal DNA-binding domain of λ cI repressor has been cocrystallized with its cognate operator, and the structure of the specific complex has been solved at 2.5-Å resolution by X-ray methods (Jordan & Pabo, 1988). The crystal structure reveals stereochemical complementarity between the helix-turn-helix (HTH) motif of λ repressor and the major groove of the cognate operator, mediated by many specific protein-DNA interactions. Related crystallographic studies of λ Cro (Brennan et al., 1990) and bacteriophage 434 repressor-operator complexes (Aggarwal et al., 1988; Wolberger et al., 1988; Mondragon et al., 1989a,b) have confirmed the generality of the HTH fold as a DNA-binding domain and have provided a detailed view of the HTH motif as a scaffold for DNA recognition. Such studies also reveal unifying features of the mechanism of HTH recognition and demonstrate the importance of detailed stereochemical interactions in lieu of a simple "recognition code" (Pabo et al., 1990; Harrison & Aggarwal, 1990; Steitz, 1990). A striking feature of the crystallographic results on phage 434 repressor-operator complexes is the different conformations of the operator in each complex, demonstrating that protein binding influences the orientation of functional groups in the major groove (Wolberger et al., 1988). This conclusion, deduced from the crystal structures, may apply also to repressor-operator complexes in solution, although direct evidence from comparison of solution structures has not yet been obtained. Since small differences in affinity between operator sites can be sufficient to define a genetic switch (Ptashne, 1986), these effects may

† Paper 43 in the series Raman Spectral Studies of Nucleic Acids. Supported by NIH Grant AI18758.
* To whom correspondence may be addressed.

0006-2960/92/0431-3118$03.00/0 © 1992 American Chemical Society

(A) O_L1 (19mer)

```
          ↓
5'   A T A T C A C C G C C A G T G G T A T   3'
3'   T A T A G T G G C G G T C A C C A T A   5'
           ↑   ↑
```

(B) N-Terminal Fragment (1-102) of λ cI Repressor

```
 1S T K K K P L T Q E Q L E D A R R L K A
21I Y E K K K N E L G L S Q E S V A D K M
41G M G Q S G V G A L F N G I N A L N A Y
61N A A L L A K I L K V S V E E F S P S I
81A R E I Y E M Y E A V S M Q P S L R S E Y E
```

FIGURE 1: (A) Sequence of the O_L1 operator (19mer). The rectangular box encloses the consensus half-site. Purines which accept hydrogen bonds in the crystal structure of a related complex with repressor (Pabo et al., 1988) are indicated by arrows. (B) Sequence of the N-terminal fragment (1–102) of λ cI repressor. The site of the Tyr88→Cys mutation is underlined.

be of central biological importance.

Positions in the O_L1 consensus half-site which have been identified in the crystal structure as binding sites for λ repressor include three purine 7N acceptors, as shown in Figure 1. Presumably an equivalent set of interactions occurs in the nonconsensus half-site, although these could not be identified in the crystal structure (Jordan & Pabo, 1988). Additionally, several hydrogen bonds are accepted by phosphate oxygens of the DNA backbone from side chains of repressor helices 2 and 3 of the HTH domain. These may facilitate proper positioning of repressor side chains (Gln44, Ser45, Asn55) which directly interact with the base pairs. Several hydrophobic interactions involving thymine methyl groups have also been implicated in binding specificity.

It is not known whether all details of binding specificity in the crystal structure of λ repressor are maintained in the solution structure. However, recent investigations of λ repressor–operator complexes by ^{15}N and ^{19}F NMR spectroscopy (Leighton & Lu, 1987; Metzler & Lu, 1989) and Raman spectroscopy (Benevides et al., 1991a,b) confirm many of the interactions observed for the crystalline HTH–DNA complexes (Benevides et al., 1991a,b). High-resolution 2D-NMR methods are expected to shed further light on solution structures of repressor–operator complexes (Weber et al., 1985; Lamerichs et al., 1988), although presently no NMR solution structure exists for the same prokaryotic complex solved by X-ray crystallography. The comparative X-ray (crystal) and NMR (solution) structure determinations of eukaryotic homeodomain–DNA complexes (Kissinger et al., 1990; Otting et al., 1990) also suggest overall similarity of HTH–DNA recognition patterns but with significant minor differences.

An alternative approach to elucidating HTH–DNA recognition in solution is to probe hydrogen-bonding interactions along the DNA major groove, especially the acceptor role of purine 7N sites and possible interactions of the pseudoacidic purine 8CH group. Purines in cognate operators of repressor and Cro proteins of phages λ and 434 are prolific in employing 7N interactions with donor groups of specific amino acid side chains (Harrison & Aggarwal, 1990). Similar 7N acceptors have been recognized in other HTH–DNA complexes (Steitz, 1990). These interactions can be investigated by monitoring the hydrogen-exchange kinetics of adenine and guanine 8CH groups using Raman spectroscopy as a dynamic probe (Benevides & Thomas, 1985).

In the present work we apply the Raman dynamic probe to examine the solution structures of complexes between the N-terminal DNA-binding domain of λ repressor (fragment 1–102, designated RF) and its cognate operator (19-base-pair O_L1 sequence). The protein and DNA sequences are shown in Figure 1. We have also employed the covalent dimer of a mutant λ repressor fragment (designated C88RF) which incorporates the mutation Tyr88→Cys and forms a Cys88–Cys88′ disulfide bridge (Sauer et al., 1986). The covalent dimer exhibits O_L1-specific operator binding, and the complex is more thermostable than that of wild type, which facilitates kinetic studies over a wide range of temperatures. Mutant complexes were prepared with 2:1 and 1:1 stoichiometry of protein monomer to DNA duplex, designated 2(C88RF):O_L1 and C88RF:O_L1, respectively. Comparative studies of both mutant and wild-type complexes are reported. These investigations characterize specific adenine and guanine deuterium-exchange rates in O_L1 in the presence and absence of repressor and permit conclusions about the major groove sites involved in repressor binding. The Raman dynamic probe complements equilibrium Raman studies of these complexes reported previously (Benevides et al., 1991a,b).

Experimental Procedures

(*1*) *Materials.* The wild-type repressor fragment (RF) and the mutant containing the substitution Tyr88→Cys (C88RF) were overexpressed in *Escherichia coli* and purified as described (Sauer et al., 1986). The purified proteins were exhaustively dialyzed against 0.05 M NH_4HCO_3 and lyophilized. Typically, aliquots containing 1 mg of protein, as determined by UV absorption spectroscopy (Graves et al., 1968), were lyophilized and resuspended in 0.1 M NaCl in D_2O (Aldrich, 99.8%) to achieve a final protein concentration of 50 mg/mL (3.8×10^{-3} M) at pD 7.8 ± 0.5. The proteins were >98% pure as determined by sodium dodecyl sulfate–polyacrylamide gel electrophoresis (SDS–PAGE). At the concentrations employed for Raman spectroscopy, the wild-type repressor fragment exists predominantly as a noncovalent dimer (Sauer et al., 1986) while C88RF is a covalent dimer. On the basis of line broadening of aromatic proton NMR resonances, the median melting temperatures of wild-type and mutant repressor fragments have been determined as 50 ± 2 and 58 ± 2 °C, respectively (Weiss et al., 1987). The 19-bp O_L1 was made by annealing the single strands 5′-d(ATACCACTGGCGGTGATAT) and 5′-d(ATATCACCGCCAGTGGTAT) in stoichiometric equivalence, as determined by UV absorption. The duplex was lyophilized and resuspended in D_2O twice to remove residual H_2O. For Raman spectroscopy, D_2O solutions of O_L1 were prepared at 25 mg/mL in 0.1 M NaCl at pD 7.8 ± 0.2.

(*2*) *Preparation of Complexes.* Repressor–operator complexes were prepared by adding the appropriate quantity of operator to a D_2O solution containing 50 mg/mL repressor in 0.1 M NaCl at pD 7.8 ± 0.5. D_2O solutions of DNA and complexes were determined to contain less than 1% HDO contamination, as judged by the absence of significant Raman band intensity in the OH stretching region (3200–3500 cm^{-1}). For the mutant repressor, complexes of both 2:1 and 1:1 stoichiometry were investigated. The 2:1 complex [2-(C88RF):O_L1], which contains two repressor "half-dimers" (i.e., one covalent dimer) per operator duplex, is predominantly (>95%) complexed material at equilibrium. The 1:1 stoichiometry (C88RF:O_L1) contains a 2-fold molar excess of DNA duplex and provides a solution in which virtually all repressor is bound to DNA, but a substantial proportion of the DNA remains protein-free. Complex formation was

verified by DNA gel retardation assays. Samples were run on a 20% acrylamide gel using a TBE buffer system (89 mM Tris + 89 mM borate + 2 mM EDTA) with O_L1 operator as a control.

(3) Incubation of Samples for Hydrogen Isotope Exchange. D_2O solutions of DNA and complexes were sealed in glass capillaries (Kimax 34507) which were employed as Raman cells. Deuterium exchange of purine 8CH groups in these samples was carried out at 40.0 °C by inserting the capillaries in a water bath (Haake, Model FE2) thermostated to within ±0.2 °C. For a given sample, duplicate runs were carried out as follows. Spectral data were collected prior to incubation (t = 0 h) and at appropriately selected time intervals between the initiation and conclusion of incubation. The total incubation period was of the order of several hundred hours at 40.0 °C. Ordinarily, the sample cell was transferred from the incubating bath to a refrigerated jacket (≤10 °C) in the spectrometer sample chamber and maintained at the low temperature to arrest exchange while spectral data were collected. Following conclusion of the data collection protocol, the sample was returned to the incubator for resumption of deuterium exchange.

(4) Data Collection and Analysis. Raman spectra at 7-cm^{-1} resolution were collected primarily on a Spex Model 1877 Triplemate spectrometer, interfaced with an EG&G-Princeton Applied Research Model 1460 optical multichannel analyzer (OMA III) and Model 1421B-1024-G cooled diode array. Samples were illuminated with the 514.5-nm line of an argon laser, using 200 mW of power at the sample. The sample temperature was maintained at or below 10 °C during data collection. Ordinarily, 100 exposures were collected with an exposure time of 40 s. The data were accumulated and averaged using commercial software routines (EG&G-PAR). Additional Raman spectra were collected on a scanning spectrometer (Spex Model 1401) operating at 8-cm^{-1} resolution. The data accumulation and averaging were carried out using Asyst software. Further details of instrumentation are described elsewhere (Lamba et al., 1990; Benevides & Thomas, 1985).

The spectral data were imported to an IBM microcomputer, baseline-corrected, normalized, and processed for difference spectroscopy using Spectra-Calc software (Galactic). The Raman band of DNA at 1090 cm^{-1} (phosphodioxy symmetric stretching mode) was used to normalize DNA intensities. The intensity of this band is invariant to both purine 8CH exchange (Benevides & Thomas, 1985) and repressor–operator complex formation (Benevides et al., 1991b). Plotting of data and statistical analysis of results were facilitated with SigmaPlot software. Further details of the application of rapid Raman data collection methods in purine 8CH exchange studies have been described (Lamba et al., 1990).

(5) Models for Purine 8CH Exchange. Hydrogen isotope exchange of the purine 8CH group follows pseudo-first-order kinetics in neutral D_2O solutions and is governed by the mechanism of eq 1 (Tomasz et al., 1972; Thomas & Livramento, 1975).

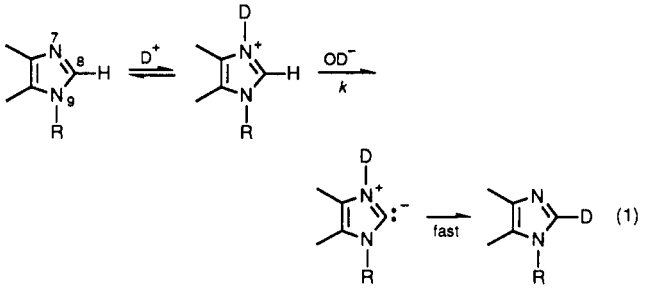

(1)

Studies of deuterium exchange of 8CH groups in nucleic acids have demonstrated sensitivity of the rate constant, k, to the macromolecular secondary structure (Benevides & Thomas, 1985). The rate is greatly affected by solvent access to the 7N–8C network and is particularly sensitive to helix groove dimensions and hydrogen bonding of the purine 7N acceptor (Benevides & Thomas, 1985) and 8CH donor (Benevides & Thomas, 1988) groups. Different microenvironments at the 7N–8C locus, including binding of protein ligands, are expected to alter the rate of 8CH exchange. The profile of purine exchange kinetics in an operator sequence can, in principle, provide an index of major-groove sites which interact specifically with repressor side chains.

In the present work we applied Raman spectrophotometry to operator DNA and repressor–operator complexes to monitor the intensity decay at Raman frequency σ of an exchange-sensitive band of initial intensity I_σ^0 (corresponding to the 8CH isotopomer) and final intensity I_σ^∞ (8CD isotopomer), following incubation of the sample in D_2O solution. The exchange rate constant k (at 40 °C) was calculated using the relation

$$k = (1/t) \ln [(I_\sigma^0 - I_\sigma^\infty)/(I_\sigma^t - I_\sigma^\infty)] \qquad (2)$$

where I_σ^t is the Raman intensity at frequency σ and time t. As shown previously, adenine (k_A) and guanine (k_G) exchange rates may be determined with eq 2 for σ = 722 and 684 cm^{-1}, respectively, while the composite rate ($k_{(A+G)}$) is determined for σ = 1485 cm^{-1} (Lamba et al., 1990). We identify two simple kinetic models (I and II) according to which the rate constants can be interpreted.

Model I. In this model it is assumed that all guanines exchange at a common rate (k_G^I), as do all adenines (k_A^I). Equation 2 then provides an average exchange rate constant for all G residues when σ = 684 cm^{-1} and for all A residues when σ = 722 cm^{-1}. The rates k_G^I and k_A^I correspond respectively to averages over all guanines and adenines in the operator sequence. Interpretation of the data according to this model provides no information on differently exchanging classes of each purine. In effect, guanines which are interacting with a ligand (e.g., a repressor side chain) are not discriminated from noninteracting G residues. Guanine–ligand interaction is revealed, for example, by a value for k_G^I which is smaller than that of guanines in ligand-free operator.

Model II. Here we assume that each guanine (or adenine) exists in one of two kinetically distinct environments—either it is free of interaction with repressor ligand or it is not. G (or A) which is noninteracting is expected to exchange identically with G (or A) of ligand-free operator. On the other hand, G (or A) which interacts with a repressor ligand is expected to resist measurable exchange. According to this model, we have four distinct classes of exchangable purines, viz., "noninteracting" G and A and "interacting" G and A, with corresponding rate constants k_G^0, k_A^0, k_G', and k_A' (where $k_G' \ll k_G^0$ and $k_A' \ll k_A^0$). Here, k_G^0 and k_A^0 are transferred from measurements on protein-free operator, while application of eq 2 yields the apparent rate constant k_G when σ = 684 cm^{-1} (or k_A when σ = 722 cm^{-1}), from which the fractions of interacting G and A can be calculated.

Procedures for application of eq 2 with σ = 1485 cm^{-1} have also been described (Lamba et al., 1990). The band at 1485 cm^{-1} is a composite of both guanine and adenine contributions, and its intensity decay provides a mean exchange rate, $k_{(A+G)}$, for all purines. With appropriate measurements and with use of nonlinear regression techniques, both k_G and k_A can be deduced from the 1485-cm^{-1} intensity decay (Lamba et al., 1990).

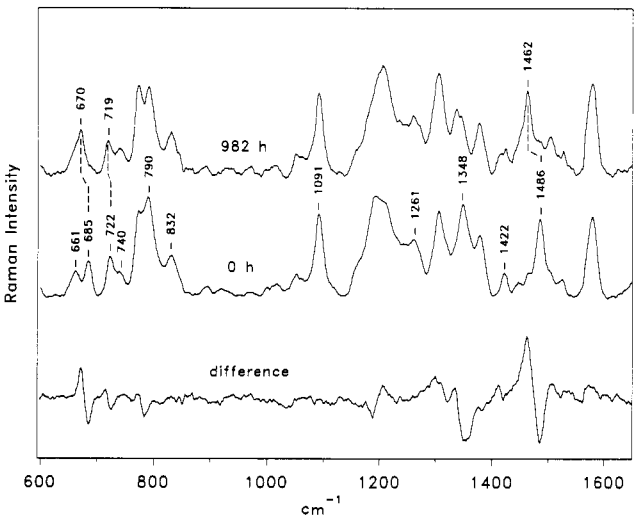

FIGURE 2: Time dependence of the O_L1 Raman spectrum reflecting purine 8CH exchange. The spectral region 600–1650 cm^{-1} is shown for O_L1 immediately after preparation of the D_2O solution (0 h, middle) and following incubation in D_2O at 40 °C to effect complete 8CH deuteration (982 h, top). The computed difference spectrum is also shown (bottom). The DNA concentration is 25 mg/mL at pD 7.8 in 0.1 M NaCl. Corresponding data for the CH stretching region, 2800–3200 cm^{-1}, have been discussed by Lamba et al. (1990).

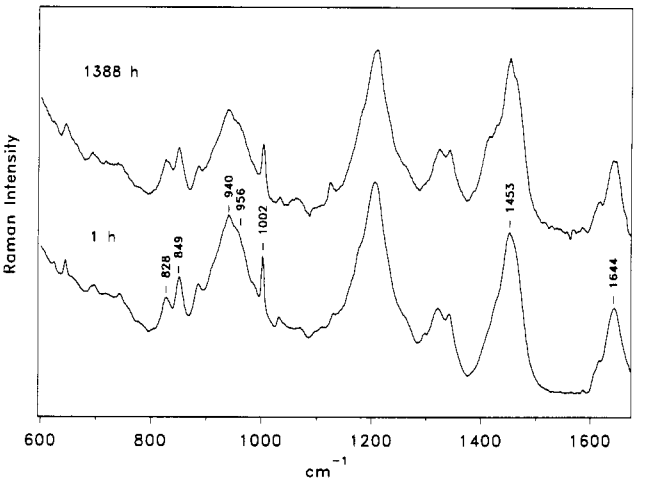

FIGURE 3: Comparison of the Raman spectra of mutant repressor C88RF shortly after preparation of a D_2O solution sample (1 h, bottom) and following prolonged incubation in D_2O at 40 °C (1388 h, top). The protein concentration is 50 mg/mL at pD 7.8 in 0.1 M NaCl.

Results and Conclusions

(1) Operator O_L1. (a) The Raman Spectrum Indicates a B-DNA Structure. The Raman spectrum (600–1650-cm^{-1} region) of O_L1 in D_2O solution is shown in Figure 2. The characteristic DNA bands which serve as conformation markers and identify the O_L1 secondary structure as that of B-DNA have been catalogued and discussed in detail for corresponding H_2O solutions (Benevides et al., 1991b). Minor differences occur in the positions of most of these DNA bands with the change of solvent from H_2O to D_2O, reflecting deuterium substitution of exocyclic amino and imino protons (Prescott et al., 1984). For D_2O solutions, the DNA conformation markers occur at 684, 722, 741, 831, 1091, and 1261 cm^{-1}, assigned respectively to dG, dA, dT, OPO, PO_2^-, and dC moieties (Prescott et al., 1984; Thomas & Wang, 1988). These establish O_L1 as right-handed B-DNA containing C2′-endo sugar pucker and anti-glycosyl torsion for all nucleosides.

(b) 8CH Exchanges of dA and dG Confirm a B-DNA Duplex. As shown in Figure 2, deuterium substitution of 8CH groups of O_L1 (i.e., 8CH → 8CD exchange) shifts the composite purine band at 1485 cm^{-1} (dG + dA) to 1462 cm^{-1}, as well as the 684-cm^{-1} (dG) and 722-cm^{-1} (dA) markers to 670 and 719 cm^{-1}, respectively, in accordance with results obtained on mononucleotides (Lane & Thomas, 1979; Thomas & Livramento, 1975) and polynucleotides (Benevides & Thomas, 1985; Lamba et al., 1990). As noted in the preceding section, the 1485 → 1462-cm^{-1} shift is most useful for monitoring the *composite* exchange of dG and dA. For protein-free O_L1 at 40 °C, the data of Figure 2 yield by eq 2 the following: $k_{(A+G)}^{op} = 0.0013 \pm 0.0002$ h^{-1}. The intensity decreases at 684 and 722 cm^{-1}, or concomitant increases at 670 and 719 cm^{-1}, which can be measured reliably using digital difference methods, permit evaluation of the exchange kinetics of dG and dA *separately* (Lamba et al., 1990). Again using eq 2, we obtain from the data of Figure 2 the following: $k_G^{op} = 0.0024 \pm 0.0003$ h^{-1} and $k_A^{op} = 0.00062 \pm 0.0004$ h^{-1}. Corresponding rate constants for the 5′-deoxyribonucleotides at 40 °C are $k_{GMP} = 0.00536$ h^{-1} and $k_{AMP} = 0.00347$ h^{-1} (K. E. Reilly and G. J. Thomas, Jr., unpublished results). Therefore, we find for O_L1 a guanine retardation factor ($R_G \equiv k_{GMP}/k_G^{op}$) of 2.2 and an adenine retardation factor ($R_A \equiv k_{AMP}/k_A^{op}$) of 5.2. These results confirm and extend to the O_L1 oligonucleotide duplex the dependence of 8CH exchange upon secondary structure (Benevides & Thomas, 1985; Lamba et al., 1990). We note also that the mononucleotide exchange rates determined experimentally at 40 °C (data not shown) are in accord with those calculated from previously determined Arrhenius parameters (Benevides et al., 1984).

Figure 2 shows significant 8C deuteration shifts in bands of the 1250–1450-cm^{-1} interval. These arise from overlapping contributions of dG and dA (Lamba et al., 1990) and provide a qualitative fingerprint of 8C deuteration. Additionally, small difference features attributable to 8C deuteration underlie the intense and overlapping bands of the DNA pyrimidines (750–800 cm^{-1}) and D_2O solvent (1180–1220 cm^{-1}).

(2) Repressor Fragment 1–102. (a) The Tyr88→Cys Mutant Repressor Fragment (C88RF) Is α-Helical. Figure 3 shows the Raman spectrum of the Tyr88→Cys mutant repressor fragment 1–102 (C88RF) in D_2O solution. The principal Raman bands of C88RF are similar to those of the wild-type fragment (RF), including amide I′ at 1644 cm^{-1} and amide III′ at 940 cm^{-1}, which indicate predominantly α-helical secondary structure (Thomas et al., 1986a). The mutant and wild-type proteins exhibit nearly identical spectra except for the intensities of bands related to Tyr88 which are diminished in the mutant. A detailed structural analysis of these Tyr88→Cys intensity differences has been given previously for H_2O solutions (Benevides et al., 1991a). The solution Raman data on C88RF are consistent with the crystal structure of wild-type repressor (Pabo & Lewis, 1982), indicating about 60% α-helical secondary structure in the N-terminal domain.

(b) The Wild-Type Repressor Structure Is Stable at 40 °C. Comparison of the Raman spectra of the wild-type repressor fragment 1–102 (RF), before and after incubation in D_2O for several hundred hours at 40 °C, reveals no significant changes in band frequencies or intensities. (See also the following section.) These results show that for RF (i) deuterium exchanges of protein NH and OH groups are rapid with respect to the time frame of purine 8CH exchanges; (ii) secondary and tertiary structures are not altered with the prolonged incubation; and (iii) the major spectral changes occurring in complexes with operator O_L1 (below) can be attributed with

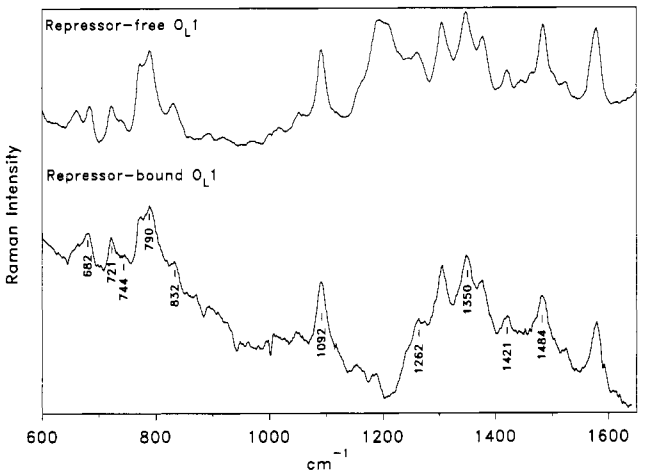

FIGURE 4: (Top) Raman spectrum of protein-free O_L1. Solvent is not compensated in this spectrum, and the D_2O band appears prominently near 1205 cm^{-1}. (Bottom) Raman spectrum (650–1600 cm^{-1}) of repressor-bound O_L1, generated by subtraction of the spectrum of the protein (C88RF) from that of the 2:1 complex [2(C88RF):O_L1]. The constituent spectra were normalized to minimize intensity differences of protein Raman bands at 1002 (Phe), 939 (amide III'), and 850 cm^{-1} (Tyr). All solvent (D_2O) bands are compensated by the subtraction procedure. The labeled bands identify key B-DNA conformation markers (Table I) of protein-free O_L1 which are conserved in the complex (cf. top spectrum).

Table I: Conformation Markers[a]

B-DNA nucleoside conformation markers			backbone conformation markers		
base	D_2O	H_2O	group	D_2O	H_2O
G	684 ± 2	682 ± 2	OPO	790 ± 3	790 ± 3
A	1350 ± 2	1339 ± 2		830 ± 2	828 ± 2
C	1265 ± 5	1255 ± 5	PO_2^-	1091 ± 1	1092 ± 1
T	661 ± 2	669 ± 2	CH_2	1422 ± 2	1422 ± 2
	743 ± 2	748 ± 2			

[a] Based upon Raman and X-ray studies of DNA oligonucleotides. Further discussion of the Raman markers and the basis for assignments is given by Thomas and Wang (1988) and references therein.

Table II: Observed Rate Constants[a] and Retardation Factors

sample	k_G (h^{-1})	k_A (h^{-1})	R_G	R_A
dGMP	0.00536		1.0	
dAMP		0.00347		1.0
CTDNA[b]	0.0031	0.00081	1.7	4.0
C88RF + CTDNA	0.0029	0.00074	2.0	4.3
O_L1[c]	0.0024	0.00062	2.2	5.2
2(C88RF):O_L1	0.00046	0.00043	11.5	7.4
2RF:O_L1	0.00050	0.00034	10.6	9.4

[a] Error limits for measured rates are within ±10% for most entries; for mononucleotides reproducibility was within ±5%. [b] Calf thymus DNA fragments of 160 base pairs. Similar data have been reported for intact calf thymus DNA (Lamba et al., 1990). [c] Similar data have been reported for operator O_R3 (Lamba et al., 1990).

confidence to hydrogen isotope exchanges in the repressor-bound operator, viz., 8CH → 8CD.

(*c*) *The Mutant Repressor Secondary Structure Is Stable at 40 °C.* Figure 3 compares the spectrum of C88RF before (lower trace) and after (upper trace) prolonged incubation at 40 °C in D_2O. No major band shifts are evident, indicating no significant deuteration of protein groups beyond that which occurs rapidly (NH → ND and OH → OD) at dissolution. The data show further that the structure of the protein is largely invariant to prolonged incubation at 40 °C. Importantly, the amide I' (1644-cm^{-1}) and amide III' (940-cm^{-1}) bands retain the positions characteristic of a predominantly α-helical secondary structure (Thomas et al., 1986a). Small intensity changes are observed near 1415 and 830 cm^{-1}. If modifications of side chains or proteolytic cleavages occur, less than 12% of the protein would appear to be affected. For example, if the intensity change at 830 cm^{-1} is attributed entirely to tyrosine, the intensity quotient I_{850}/I_{830} is decreased by only 11%. Similarly, the intensity change near 1415 cm^{-1} represents about 10% of the total 1450-cm^{-1} band intensity. PAGE also indicates that most of the incubated C88RF protein migrates with the same mobility as nonincubated protein. The Raman spectrum and structure of C88RF, like those of RF, are essentially conserved with incubation at 40 °C. Significantly, no major changes occur in the protein Raman background for those regions of the spectrum coinciding with exchange-sensitive bands of DNA, viz., 1465–1485, 715–730, and 660–690 cm^{-1}. Finally, we note that the structure of the mutant repressor in complexes with O_L1 is even more robust to prolonged incubation at 40 °C (see below), which shows that the stability of C88RF is enhanced in complexes with O_L1. This is consistent with NMR spectra of C88RF and its complexes (M. A. Weiss, personal communication).

(*3*) *Mutant Repressor–Operator Complexes.* (*a*) *The B-DNA Structure of O_L1 Is Conserved with Repressor Binding.* Figure 4 compares the Raman spectra of D_2O solutions of protein-free O_L1 and repressor-bound O_L1 [complex 2-(C88RF):O_L1]. The latter was obtained by subtracting the D_2O solution spectrum of C88RF from that of the 2-(C88RF):O_L1 complex. The computed difference spectrum shows that the B-DNA marker bands of O_L1 are essentially invariant to mutant repressor binding. Specifically, the C2'-endo/anti nucleoside markers [684 (G), 722 (A), 741 (T), and 1261 cm^{-1} (C)] and phosphodiester marker (832 cm^{-1}) are as expected for B-DNA in D_2O (Table I). Also, subtraction of the spectrum of O_L1 from that of 2(C88RF):O_L1 showed no difference bands that could be attributed to a significant change in protein secondary structure with complex formation, in agreement with previously reported H_2O solution studies (Benevides et al., 1991b). Similar results were obtained for the 1:1 complex, C88RF:O_L1 (data not shown).

(*b*) *Repressor Binding Retards 8CH Exchanges in O_L1.* The Raman spectrum of 2(C88RF):O_L1 in D_2O solution is expected to change as deuterium substitution of purine 8CH groups progresses. The spectral interval 600–1150 cm^{-1}, which contains the principal markers of 8CH exchange, is shown in Figure 5 as a function of time of incubation in D_2O at 40 °C. The band shifts, 684 → 670 cm^{-1} and 722 → 719 cm^{-1}, indicate 8C deuterations of dG and dA, respectively. Comparison of the data of Figures 2 and 5 shows that 8C exchanges in the complex are much slower than in the free operator. Semilogarithmic plots of intensity vs time are shown in Figure 6 for O_L1 and the 2(C88RF):O_L1 complex. The calculated rate constants (eq 2) are given in Table II. Rate constants for the 2:1 complex (k_G^{cx2} = 0.00046 ± 0.00002 h^{-1} and k_A^{cx2} = 0.00043 ± 0.00003 h^{-1}) provide retardation factors R_G^{cx2} = 11.5 and R_A^{cx2} = 7.4, respectively. Thus, repressor binding in the 2:1 complex retards 8CH exchange of dG by an additional factor of 5 and of dA by an additional factor of 1.5 over values observed for free O_L1. These "repressor-induced retardation effects" are also seen in the 2(RF):O_L1 complex for which k_G^{cx2} = 0.00050 ± 0.00005 h^{-1} (R_G^{cx2} = 10.6) and k_A^{cx2} = 0.00034 ± 0.00003 h^{-1} (R_A^{cx2} = 9.4). Again dG is exchanged about 5 times more slowly and dA about 2 times more slowly than in protein-free O_L1.

Frequency shifts, similar to those discussed above for the protein-free operator, are also observed in the 1250–1500-cm^{-1}

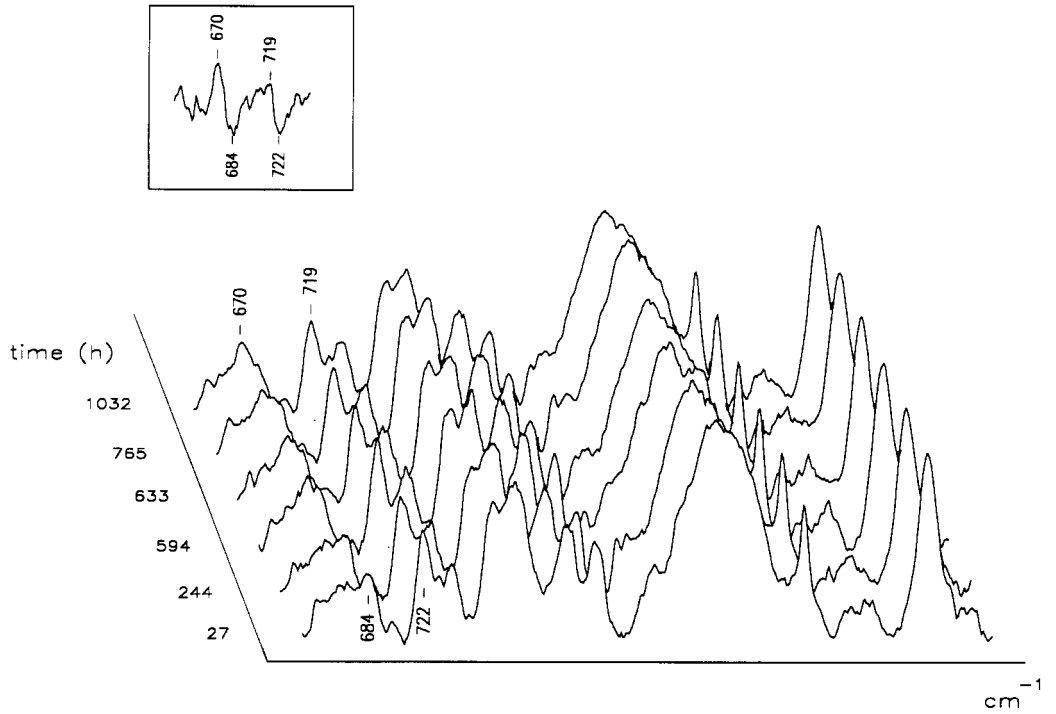

FIGURE 5: Series of spectra in the region 600–1150 cm^{-1} of the 2:1 complex of mutant repressor [2(C88RF):O_L1] obtained over a 1000-h period of incubation. The spectra show time-dependent changes in the 8CH-exchange-sensitive Raman bands of dG (684/670 cm^{-1}) and dA (722/719 cm^{-1}). The inset (upper left) displays a 2-fold amplification of the 600–800-cm^{-1} region of the difference spectrum between 1032 and 27 h.

spectral region of repressor–operator complexes. As before, these are attributed to 8C deuteration of purines (Lamba et al., 1990). The composite exchange rate $k_{(A+G)}$, calculated from the intensity decrease at 1480 cm^{-1}, is consistent with the results of Figure 6, reported in Table II.

(*c*) *O_L1 Binding Enhances Repressor Thermostability.* We find no significant changes in the region 1400–1430 cm^{-1} of the Raman spectrum of the 2(C88RF):O_L1 complex following prolonged incubation (>1000 h) in D_2O. This contrasts with the DNA-free protein which exhibits a weak 1415-cm^{-1} band (Figure 3). We conclude that the thermostability of C88RF is enhanced in complexes with O_L1. The estimated >88% retention of native structure in the noncomplexed repressor is increased to virtually 100% in the complex with O_L1.

(*d*) *Retardation Indicates Specific Repressor–Operator Binding.* The kinetic results presented above establish that binding of the N-terminal domain of λ repressor to O_L1 restricts D_2O solvent access to purine major-groove sites. Since the O_L1 secondary structure remains that of B-DNA with repressor binding (Figure 4), the retardation of 8CH exchange cannot be attributed simply to a change in DNA backbone conformation. Further, parallel experiments carried out on mixtures of repressor with nonoperator DNA (calf thymus nucleohistone DNA fragments of 160 bp) showed no significant retardation of guanine 8CH exchange and only residual retardation of adenine 8CH exchange (Table II). Therefore, we conclude that the retardations observed in repressor–operator complexes are due to *operator-specific* repressor binding, rather than to nonspecific association of protein and DNA.

(*e*) *Correlation with the Number of Interacting Purine Residues.* For the 2:1 complex [2(C88RF):O_L1], theoretically all operator binding sites can be occupied. DNase protection studies on mutant repressor–operator complexes indicate for λ operator $K_d = 3.0 \times 10^{-8}$ M (Sauer et al., 1986), which implies that the equilibrium concentration of unbound operator constitutes less than 5% of the DNA in the 2:1 mixture. In the following section we interpret the rate data on the assumption that the solutions contain, at equilibrium, predominantly repressor-bound DNA, in accordance with the mea-

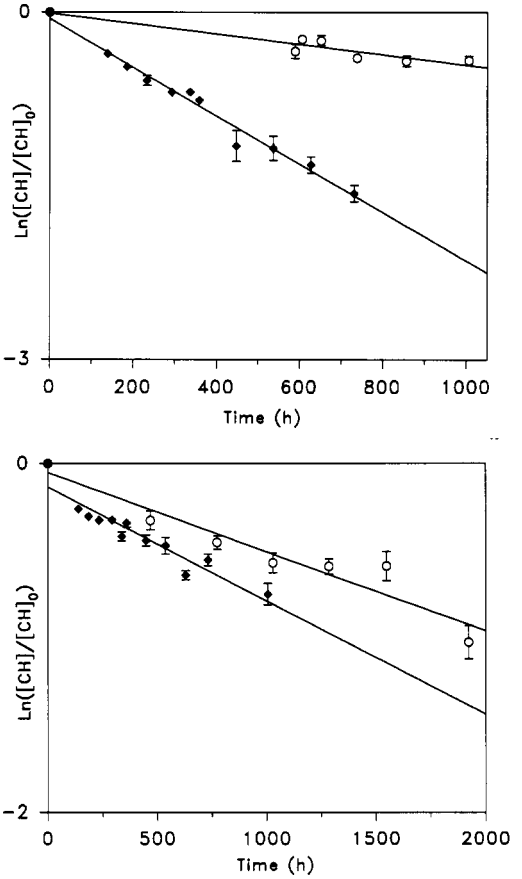

FIGURE 6: Semilogarithmic plots of the intensities of the guanine 684-cm^{-1} band (top) and adenine 722-cm^{-1} band (bottom) vs time of exchange in D_2O at 40 °C for O_L1 (◆) and 2(C88RF):O_L1 (○). Error limits for the data points are within the sizes of the symbols, except where indicated otherwise.

sured dissociation constant. This approach is consistent with our observation that a 3:1 mixture, which contains more than the stoichiometric equivalent of one repressor "dimer" per duplex, showed only marginal differences from the 2:1 mixture with respect to 8CH exchange rates.

Discussion and Summary

(*1*) *Model I: Interpretation of Average Rate Constants.* We have defined two simple models for interpreting operator exchange kinetics. (See Experimental Procedures, Section 5, above.) According to model I, average rate constants, k_A^I and k_G^I, are assigned to dA and dG residues, respectively. Repressor–operator interactions are presumed to depress k_A^I and/or k_G^I with respect to rates observed for protein-free operator. The magnitude of rate constant depression is expected to be a quantitative measure of repressor–operator interaction involving major groove sites. In accordance with this model, the results of Table II indicate the following: (i) Interaction of repressor with major-groove sites is always greater for operator DNA (O_L1) than for nonoperator DNA (calf thymus fragments). (ii) Operator-specific binding occurs for both wild-type repressor and the Tyr88→Cys mutant repressor. (iii) In both wild-type and mutant complexes depression of k_A^I is less than that of k_G^I, implying gross similarity of protein–DNA interactions in the two complexes. (iv) In the repressor–operator complexes, the depressions of k_G^I and K_A^I are comparable to those observed for protein-free nucleic acids (RNA) in the A-form (Benevides & Thomas, 1985). Therefore, repressor binding to B-DNA is at least as effective in sequestering solvent from the 7N–8C loci of purines as that which results from withdrawal of the bases deeply within the major groove. *We imply no structural similarity between repressor-bound O_L1 and the geometry of A-DNA.* We point out only that comparable retardations of purine 8CH exchange are observed in both cases. (v) Finally, as will be further discussed in the following section, the data of Table II imply that both steric shielding and hydrogen bonding by repressor donor groups (to 7N acceptors) contribute to the retardation of operator 8CH exchange.

(*2*) *Model II: Resolution of Different Purine Classes.* The present results are more usefully interpreted in terms of model II, which defines two classes of guanines and adenines, viz., those which undergo exchange at the same rates as purines in protein-free DNA (repressor-free fraction, f^0) and those which undergo no exchange (repressor-bound fraction, f'). With X = A or G, we represent the effective rate constants in accordance with earlier notation as $k_X^{II} = f_X^0 k_X^0 + f_X' k_X'$. Since $f_X^0 + f_X' = 1$, and by assumption, $k_X' = 0$, the data of Table II may be used to calculate the fractions of protein-bound purine, $f_X' = 1 - k_X^{II}/k_X^0$. Accordingly, we obtain for the 2(C88RF):O_L1 complex $f_G' = 0.81$ and $f_A' = 0.31$. These values correspond to restriction from 8CH exchange of 7 guanines and 3 adenines per O_L1 duplex in the mutant repressor complex. For the wild-type complex, 2(RF):O_L1, the data of Table II indicate restriction from 8CH exchange of 7 guanines and 5 adenines.

(*3*) *Relation to Other Structural Studies.* Further discussion of these results in relation to structural (Jordan & Pabo, 1988) and biochemical studies (Pabo et al., 1982) of repressor–operator complexes is of interest. X-ray crystallography of the complex of wild-type repressor (fragment 1–92) with O_L1 (17mer) has been reported (Jordan & Pabo, 1988). The crystal structure reveals several interactions between protein side chains and major-groove sites of the bases. Specifically, 7N of A2, G12′, and G14′ in the consensus half-site (Figure 7) are proposed as accepting hydrogen bonds

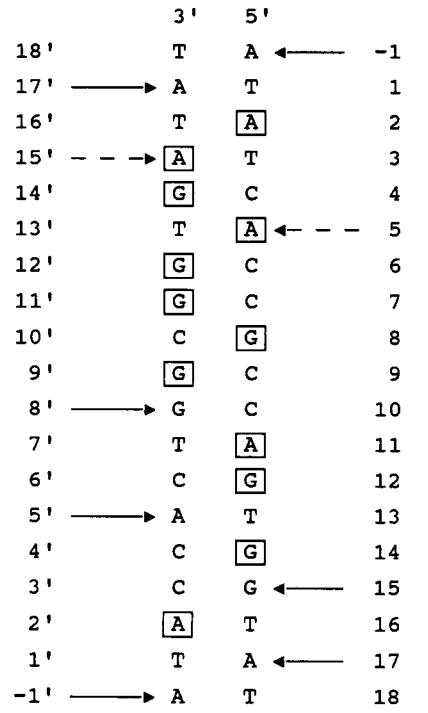

FIGURE 7: Purine 8CH exchange profile of O_L1 in repressor complexes. Schematic diagram showing the proposed purine 8CH exchange profiles of O_L1 operator in complexes with wild-type and mutant repressors. Boxes indicate purines which are protected, and arrows indicate purines which are unprotected from 8CH exchange in the wild-type complex. Broken arrows indicate additional residues which, though protected in the wild-type complex, are proposed to be unprotected in the mutant complex.

from side chains Gln44, Ser45, and Asn55, respectively. Assuming analogous interactions in the nonconsensus half-site, 6 of the 17 purines per duplex should be directly involved in 7N hydrogen bonding. In the crystal structure, the bound repressor also makes close contacts to 7N sites of two purines which are near the central operator domain, G11′ and A11. Accordingly, it is likely that 7N sites of G11′ and A11 are also solvent-shielded. Therefore, the crystal structure of repressor-bound O_L1 allows for hindered 8CH exchange of at least 8 purines (5 guanines + 3 adenines). In addition to the crystal structure results, Pabo and co-workers (1982b) demonstrated through methylation footprinting that G8 and G9′ are also shielded. The repressor N-terminal side chains (Ser1-Thr2-Lys3-Lys4-Lys5) implicated in the methylation protection experiments are not visualized in the "room-temperature" X-ray structure due presumably to disorder of the N-terminus in the crystal. However, these residues are visualized in a low-temperature (−15 °C) crystal structure, which reveals contacts of Lys3 and Lys4 with operator guanines (Clarke et al., 1991). Altogether, the crystal structure and methylation protection studies suggest that at least 7 guanines and 3 adenines should exhibit some degree of retardation of 8CH exchange in our complexes. This is precisely what we observe for the mutant complex, 2(C88RF):O_L1. For the wild-type complex, 2(RF):O_L1, our data are consistent with retardation of exchange of at least 2 additional adenines. We assign A15′ and A5 as the additional adenines on the basis of proximity to major-groove sites which are solvent-shielded in the crystal structure by hydrophobic contacts involving their paired thymines (T3 and T13′) with repressor side chains (Ala49 + Ile54 and Ser45 + Gly46, respectively). These conclusions are summarized in Figure 7.

The differences observed in the exchange profiles of wild-type and mutant complexes are significant, and we attribute

them to differences in geometry of the complexes. These findings provide independent evidence for the importance of detailed sterochemical complementarity, rather than a simple DNA–protein recognition code, in accounting for interaction of repressor HTH domains with cognate operators. A similar conclusion has been reached from detailed analysis of the Raman band shifts in equilibrium studies of repressor–operator complexes (Benevides et al., 1991a,b). Overall, our results indicate that λ repressor–operator complexes in solution share many of the structural and mechanistic features proposed for crystalline complexes (Harrison & Aggarwal, 1990). A schematic model for the repressor–operator complex consistent with the available structural data and showing the exchange-sensitive purines is given in Figure 7. Future experiments will focus on the study of additional mutants to further characterize solvent access to specific major-groove sites.

ACKNOWLEDGMENTS

We are appreciative of the interest and assistance provided by Dr. James M. Benevides, University of Missouri—Kansas City, throughout this project. We thank Dr. Michael A. Weiss, Harvard Medical School, for purification of protein samples and comments on the manuscript.

REFERENCES

Aggarwal, A. K., Rodgers, D. W., Drottar, M., Ptashne, M., & Harrison, S. C. (1988) *Science 242*, 899–907.

Benevides, J. M., & Thomas, G. J., Jr. (1985) *Biopolymers 24*, 667–682.

Benevides, J. M., & Thomas, G. J., Jr. (1988) *Biochemistry 27*, 3868–3873.

Benevides, J. M., LeMeur, D., & Thomas, G. J., Jr. (1984) *Biopolymers 23*, 1011–1024.

Benevides, J. M., Weiss, M. A., & Thomas, G. J., Jr. (1991a) *Biochemistry 30*, 4381–4388.

Benevides, J. M., Weiss, M. A., & Thomas, G. J., Jr. (1991b) *Biochemistry 30*, 5955–5963.

Brennan, R. G., Roderick, S. L., Takeda, Y., & Matthews, B. W. (1990) *Proc. Natl. Acad. Sci. U.S.A. 87*, 8165–8169.

Clarke, N. D., Beamer, L. J., Goldberg, H. R., Berkower, C., & Pabo, C. O. (1991) *Science 254*, 267–270.

Graves, W. E., Davis, F. C., & Sells, B. H. (1968) *Anal. Biochem 22*, 195–210.

Harrison, S. C., & Aggarwal, A. K. (1990) *Annu. Rev. Biochem. 59*, 933–969.

Jordan, S. R., & Pabo, C. O. (1988) *Science 242*, 893–899.

Kissinger, C. R., Liu, B., Martin-Blanco, E., Kornberg, T. B., & Pabo, C. O. (1990) *Cell 63*, 579–590.

Lamba, O. P., Becka, R., & Thomas, G. J., Jr. (1990) *Biopolymers 29*, 1465–1477.

Lamerichs, R. M. J. N., Bolens, R., van der Marel, G. A., van Boom, J. H., Kaptein, R., Buck, F., Fera, B., & Rüterjans, H. (1989) *Biochemistry 28*, 2985–2991.

Lane, M. J., & Thomas, G. J., Jr. (1979) *Biochemistry 18*, 3839–3846.

Leighton, L., & Lu, P. (1987) *Biochemistry 26*, 7262–7271.

Metzler, W. J., & Lu, P. (1989) *J. Mol. Biol. 205*, 149–164.

Mondragon, A., Wolberger, C., & Harrison, S. C. (1989a) *J. Mol. Biol. 205*, 179–188.

Mondragon, A., Subbiah, S., Almo, S. C., Drottar, M., & Harrison, S. C. (1989b) *J. Mol. Biol. 205*, 189–200.

Otting, G., Qian, Y. Q., Biletter, M., Muller, M., Affolter, M., Gehring, W. J., & Wuthrich, K. (1990) *EMBO J. 9*, 3085–3092.

Pabo, C. O., & Lewis, M. (1982) *Nature 298*, 443–447.

Pabo, C. O., Krovatin, W., Jeffrey, A., & Sauer, R. T. (1982) *Nature 298*, 441–443.

Pabo, C. O., Aggarwal, A. K., Jordan, S. R., Beamer, L. J., Obeysekare, U. R., & Harrison, S. C. (1990) *Science 247*, 1210–1213.

Prescott, B., Steinmetz, W., & Thomas, G. J., Jr. (1984) *Biopolymers 23*, 235–256.

Ptashne, M. (1986) *A Genetic Switch*, Cell and BSP Press, Cambridge, MA.

Sauer, R. T., Hehir, K., Stearman, R. S., Weiss, M. A., Jeitler-Nilsson, A., Suchanek, E. G., & Pabo, C. O. (1986) *Biochemistry 25*, 5992–5998.

Steitz, T. A. (1990) *Q. Rev. Biophys. 23*, 205–280.

Thomas, G. J., Jr., & Livramento, J. (1975) *Biochemistry 14*, 5210–5218.

Thomas, G. J., Jr., & Wang, A. H.-J. (1988) *Nucleic Acids Mol. Biol. 2*, 1–30.

Thomas, G. J., Jr., Prescott, B. and Benevides, J. M. (1986) *Biomol. Stereodyn. 4*, 227–254.

Tomasz, M., Olson, J., & Mercado, C. M. (1972) *Biochemistry 11*, 1235–1241.

Weber, P. L., Wemmer, D. E., & Reid, B. R. (1985) *Biochemistry 24*, 4553–4562.

Weiss, M. A., Pabo, C. O., Karplus, M., & Sauer, R. T. (1987) *Biochemistry 26*, 897–904.

Wolberger, C., Dong, Y., Ptashne, M., & Harrison, S. C. (1988) *Nature 335*, 789–795.